ICAS-88-2.3.3 APPLICATION OF INTEGRATED FLUID-THERMAL-STRUCTURAL ANALYSIS METHODS

Allan R. Wieting*, Pramote Dechaumphai**, and Kim S. Bey**
NASA Langley Research Center
Hampton, Virginia
USA

Earl A. Thornton♠
Old Dominion University
Norfolk, Virginia
USA

Ken Morgan♠♠
University of Wales
Swansea
United Kingdom

Abstract

Hypersonic vehicles operate in a hostile aerothermal environment which has a significant impact on their aerothermostructural performance. Significant coupling occurs between the aerodynamic flow field, structural heat transfer, and structural response creating a multidisciplinary interaction. Interfacing state-of-the-art disciplinary analysis methods is not efficient, hence interdisciplinary methods integrated into a single aerothermostructural analyzer are needed. The NASA Langley Research Center is developing such methods in an analyzer called LIFTS, an acronym for Langley Integrated Fluid-Thermal-Structural analyzer. The evolution and status of LIFTS is reviewed and illustrated through applications.

Introduction

Design of lightweight structures and thermal protection systems for hypersonic vehicles depends on accurate prediction of the aerothermal loads, structural temperatures and their gradients, as well as structural deformations and stresses. Traditionally, an aerodynamicist predicts the surface pressure and heating rate assuming a rigid isothermal body. The aerodynamic heating rate is used by a structural heat transfer analyst to predict the structural temperature distributions. Finally, a structural analyst uses the temperature distributions and aerodynamic pressures to predict the structural deformations and stresses. Such a traditional independent approach requires several iterations between the different analysis methods and analysts. The approach is relatively inefficient because the incompatible mathematical models require extensive postprocessing to transfer data. Moreover, the interdisciplinary coupling and interactions, which are significant, are rarely addressed because the iterative process not only requires several additional solutions, but also remodeling in each analysis. An integrated multidisciplinary analysis procedure is required for accurate, timely prediction of the coupled response. The coupling occurs primary through the thermal response of the structure, because (1) the surface temperature affects the external flow by changing the amount of energy absorbed by the structure, and (2) the temperature gradients in the structure result in structural deformations which alter the flow field and attendant surface pressures and heating rates.

To meet the analysis requirements for hypersonic vehicles the NASA Langley Research Center is developing an Integrated Fluid-Thermal-Structural (LIFTS) analyzer using finite element methods. The method is illustrated in Fig. 1 on an actively cooled structure. A general automated unstructured gridding is used to discretize the aerodynamic and coolant flow field and the structure for the thermal and structural analyses. Currently a single nonlinear finite-element algorithm provides the solution for the environment, loads, and response for all three disciplines. The flow field computational domain is adaptively refined based on flow field error indicators to minimize grid points and increase accuracy. Several graphic techniques are used to display the results.

This paper covers the historical development, status, and plans of the integrated finite-element fluid-thermal-structural methodology in LIFTS as graphically illustrated in Fig. 2. The development of a finite element thermal analyzer equivalent to standard finite difference thermal analyzers was initiated in the mid 1970's with the development of radiation, forced convection and conduction elements and interfaced with a structural analyzer (References are referred to in detail in the text.). The next step was the development of hierarchical thermal elements with nodeless variables and an integrated thermal-structural analyzer which eliminated the post processing interface. At this point the integrated thermal structural analyzer was interfaced with existing computational fluid dynamic analyzers and the development of an integrated fluid-thermal-structural analyzer initiated. Recent research has focused on the development of efficient algorithms, adaptive refinement techniques and aposteriori error estimates for the solution of the two and three dimensional Euler and Navier Stokes equations for the computational fluid dynamics portion of the integrated fluid-thermal-structural methodology. The latter effort led to the development of the Taylor-Galerkin algorithm which is applied in conservation form for all three disciplines in LIFTS. The algorithm development for the inherently nonlinear fluid equations led to unexpected benefits in the solution of nonlinear thermal and structural (plasticity and large deformations) behavior. Salient features of various problems are used to illustrate the benefits of

*Head, Aerothermal Loads Branch, Loads and Aeroelasticity Division, Member AIAA
**Aerospace Technologist, Aerothermal Loads Branch, Loads and Aeroelasticity Division, Member AIAA
♠Professor, Department of Mechanical Engineering and Mechanics, Associate Fellow AIAA
♠♠Reader, Department of Civil Engineering, University of Wales, Swansea, Member AIAA

certain approaches and to provide insight into methodology decisions.

Evolution of Integrated Fluid-Thermal-Structural Methodology

Interfaced Thermal-Structural Analysis

In the mid 1970's, NASA developed the airframe integrated supersonic combustion ramjet shown in Fig. 3. Tests demonstrated that the fixed geometry engine, which uses the airframe forebody as part of the inlet and the afterbody as part of the nozzle, could deliver positive thrust over a Mach 6 to 10 range. Standard disciplinary methods were used to independently determine the aerodynamic loads, the thermal response, and structural performance of the hydrogen cooled concept[1].

The surface pressure and heating rates were determined assuming a rigid isothermal body. These aerodynamic heating rates were used to predict the structural temperature distributions using a finite difference electrical analog procedure (MITAS[2]). Finally, the temperature distribution and aerodynamic pressures were used to predict the structural deformations and stresses using NASTRAN[3]. Even though thermal stresses and deformations were significant, the solution was not iterated to account for coupling between the flow field and the surface deformations and temperature[4].

This thermal stress dominated problem emphasized the need for efficient methods of transferring temperature distributions to the structural model for the thermal stress analysis. The standard approach of interfacing two different codes was extremely inefficient[5]. Extensive postprocessing was required to interpolate and/or extrapolate temperature data from the thermal model to the structural model. Because of the different mathematical models and analysis methods, models with exactly the same nodal placement was impractical[5]. In fact, one of the greatest shortcomings in the thermal analysis was the lack of the automated model generation capability that existed for the finite element structural analysis[6].

Existing finite element thermal analyzers were limited to conduction, convection to a known temperature, and radiation to space[6]. Hence, new finite element thermal methodology[7-15] for mass transport, surface convection to an unknown temperature, and internal radiation[13] were developed. The new elements developed for the thermal analysis of an actively cooled engine strut[1] are shown in Fig. 4. Several comparative studies demonstrated that the finite element procedure was equivalent or better than the finite difference lumped parameter approach[7-15]. One such example, shown in Fig. 5, compares the predicted aerodynamic skin temperature and coolant temperature along the engine strut. The initial comparison with approximately 3000 node MITAS and NASTRAN thermal models highlighted the benefits of the finite element model generation capability, which not only reduced the time to construct a model but facilitated the verification of the model[6]. Current finite difference thermal analyzers do not have this severe shortcoming as finite element model generation capability has been exploited to construct thermal models. However, separate thermal and structural codes still require interfacing and interpolation of the temperature field to the structural model for the thermal stress analysis.

Even with finite element thermal and structural analyzers, an incompatibility remained[7] between thermal and structural models as shown in Fig. 6. The thermal model of a section through the strut wall is shown on the left. The cooling jacket consists of an aerodynamic skin and fins with hydrogen as a coolant. This section is modelled with conduction, convection, and mass transport elements for the thermal analysis but is ignored in the stress analysis as the the cooling jacket deforms plastically and adds negligible stiffness to the load carrying primary structure[1,4,6,7]. The primary structure consists of the wall, modelled with a quadrilateral conduction/convection element and a rib modelled with a rod conduction/convection element. The primary structure has a thermal gradient along its length and through the thickness, which creates the thermal stress field. The optimal (minimum unknowns) thermal stress model, shown on the right, consists of a beam bending element and an axial member. The beam bending element requires the average wall temperature and through the wall temperature gradient, which are not generated by the thermal model. Hence, even with the same numerical methodology incompatibilities can exist between thermal and structural models. This incompatibility could be removed by compromising the structural model (increasing the number of unknowns) and using quadrilateral membrane elements with the same nodal locations as the thermal model.

Integrated Thermal-Structural Analysis

Compatibility between the thermal and structural models is not always achievable without severely compromising the efficiency of one or both of the solutions. For instance, a structural member that carries only an axial load could be modelled with a single finite element. However, if the member has an axial temperature gradient, several linear thermal elements may be required to accurately predict the temperature gradient in the element. If the structural model had the same nodal locations as the thermal model then the data transfer would be straight forward. However, the interior nodes would have to be constrained, so as not to act as hinges, for the structural analysis. These types of incompatibilities led to the development of hierarchical thermal elements with nodeless variables[16-20]. Nodeless variables were used to obtain a higher order polynomial interpolation function without adding nodes—particularly nodes not required by the structural analysis.

The hierarchical integrated thermal-structural analysis method that evolved[20] is illustrated in Fig. 7. The example problem is a wing section with non-uniform heating (q) to the upper surface. The analysis approach,

shown on the right of the figure, is discussed below. A common discretization is used to suit the geometry, as shown in the upper left of the figure. The hierarchical thermal analysis initially assumes the temperature distribution to be linear producing the the bilinear result labelled $P_T = 1$, 2 FE (first order polynomial for element temperature distribution, two finite elements as shown on surface). An increase in the thermal polynomial to second order ($P_T = 2$) yields the nonlinear distribution labelled $P_T = 2$, 2 FE. A traditional analysis would have increased the number of linear finite elements to ten to achieve equivalent accuracy as shown ($P_T = 1$, 10 FE). The nodeless variable essentially floats so that one need not know or guess apriori the temperature distribution in order to locate elements. Hence increased accuracy is achieved without remodelling.

The next step in the hierarchical integrated thermal-structural analysis is the transfer of the thermal data to the structural analysis. This step is crucial and missing in interfaced analyses. That is, the conversion of the temperature field to equivalent thermal forces requires the same interpolation function used in the thermal analysis or, in other words, consistent thermal forces. If we ignored this step and transferred only nodal temperatures and then calculated the equivalent thermal forces with a linear interpolation function we would get a bilinear thermal stress distribution as shown by $P_S = 1$ $P_T = 1$, 2 FE. (For this analysis, bilinear, $P_S=1$, structural elements were adequate.) However by using the appropriate interpolation functions the nonlinear stress field indicated by $P_S = 1$, $P_T = 2$, 2 FE is obtained. If the domain is modelled traditionally with ten linear elements ($P_S = 1$, $P_T = 1$, 10 FE) then the nonlinear stress distribution is obtained but prediction is only fair compared to the hierarchical prediction. The discontinuities occur at the nodes indicating a coarse grid.

Shuttle Flow-Thermal-Structural Analysis Experience

A major example of the difficulty in performing a complete flow-thermal-structural analysis without integrated methods was the Space Shuttle. The aerodynamicist provided pressure and heat transfer rates over the mission profile. The thermal analysis of the Shuttle was then performed using local three dimensional plug models[5] as indicated by the solid areas in Fig. 8. Each thermal model, which consisted of approximately 200 degrees of freedom (dof), provided temperatures that had to be interpolated or smeared longitudinally and circumferentially to the structural nodal locations. Post flight evaluation of this procedure showed that the interpolation or smearing led to large discrepancies in the temperature levels and gradients, hence underprediction of the thermal stresses and deformations. One such evaluation[21] used a complete cross section of the wing as shown in Fig. 9. A comparison in Fig. 10 of the interpolated temperatures and the results from a more detailed finite element thermal model illustrates the noted discrepancies.

In addition to the models being coarse, the complete load cycle for a given mission took approximately one calender year. With this lengthy cycle, designs tended to be frozen early and any modifications were also very costly. More efficient methods that could reduce the time to perform a load cycle analysis were obviously needed. The underlying goal of the integrated fluid-thermal-structural methodology is to reduce a load cycle calculation without compromising disciplinary results.

Integrated Fluid-Thermal-Structural Analysis

Fluid Algorithms and Adaptive Procedures

The next step was the addition of the fluid module to complete the desired integrated fluid-thermal-structural analysis methodology. Some investigators modified structural finite element algorithms for fluid analysis and concluded that finite element techniques were inferior to existing finite difference procedures[22]. The approach taken herein was to exploit all the finite difference technology in the development of new finite element algorithms for computational fluid dynamics[23-30]. This led to the on going development of several algorithms (See Fig 2.) such as the Taylor-Galerkin method of Morgan[23,25] and the Petrov-Galerkin method of Hughes[31].

The Taylor-Galerkin procedure is similar to a Lax-Wendroff finite difference algorithm. A Taylor series expansion is used to obtain recurrence relationships to march the solution in time. The Galerkin criteria is used to obtain the spatial discretization of the domain. Application of the Taylor-Galerkin algorithm to benchmark problems demonstrated accuracy and efficiency[23,24,26,27]. Several of these problems required capturing shock waves and high thermal gradients near the surfaces. Since finite element thermal and structural methods traditionally used unstructured grids to transition from coarse to fine meshes in order to capture gradients, it was natural to consider unstructured meshes for the fluid domain. Although this was considered unorthodox by the finite difference community, adaptive unstructured methods were developed by Peraire and Morgan[25,29] and Ramakrishnan, Bey, and Thornton[30] with great success. The adaptive remeshing procedure of Peraire et. al.[25,29] uses only triangles and adapts the mesh based on error indicators of flow variables such as density and temperature. Ramakrishnan, et. al.[30] developed a mesh enhancement procedure using triangles to transition between coarse and fine quadrilateral meshes. They also used flow error indicators to adaptively enhance the mesh where required. Both procedures remove mesh points where unnecessary, hence obtaining near optimal meshes for the problem at hand.

The adaptive unstructured remeshing scheme of Peraire is illustrated in Fig. 11. The schlieren photograph on the left of Fig. 11 shows an incident oblique shock wave intersecting the bow shock wave of a cylinder immersed in a Mach 8 flow. This interaction results in a shock interference pattern, classified by Edney[32] as a Type IV supersonic jet, that impinges on the cylinder surface. The final unstructured mesh adapted to the flow physics[27] is shown in the right of

Fig. 11. Note that the mesh density gradient simulates the flow density gradient given by the schlieren. The planar boundaries of the mesh encompass the flow domain and the circular part the cylinder. The solution is initiated on a relatively uniform mesh. The initial mesh and subsequent meshes are remeshed periodically (about three times) based on density error indicators until the solution converges. The lower part of Fig. 11 shows an enlargement of the shock front to illustrate that the element base is oriented parallel to the maximum gradient (perpendicular to the shock). The triangle dimensions are a function of the error indicators, which are a function of the gradient. Hence, if the second principle gradient is small the user can allow high aspect ratio elements (equality of error indicators in the principal directions) to decrease the problem size.

The shock wave interference problem illustrated above is a formidable thermal-structural design issue for hypersonic vehicles with airbreathing engines[34-35]. The incident shock is generated by the vehicle nose or compression ramps on the undersurface of the vehicle which acts to precompress the air flow passing into the engine as illustrated in Fig. 12. Aerodynamicist design for this shock-on-lip condition to maximize the compressed air flow into the engine and hence performance. The experimental configuration in the lower left of Fig. 12, which simulates the vehicle forebody and cowl leading edge, was used to define the aerothermal loads[34-35]. The schlieren photograph shows a supersonic jet interference pattern impinging on the surface of the cylinder. The interference pattern produces intense local amplification of the pressure and heat transfer in the vicinity of the jet impingement. The undisturbed (absence of incident shock) stagnation point pressure and heating rate can be amplified by factors from 6 to 30 depending on the shock strength and free stream Mach number[34-35].

This experimental data was used to calibrate the finite element solution and adaptive meshing techniques. Both adaptive unstructured grid techniques performed well[27,28,30]. However, the Taylor-Galerkin algorithm when applied to meshes with triangular and quadrilateral elements was found to be unstable at the transition nodes[30]. A Runge-Kutta finite element algorithm proved effective for these meshes[30]. The triangular remeshing procedure does not have the stability problems although it can have dispersion errors for large aspect ratio elements[30].

The severe gradients in the jet impingement region required extremely fine meshes to resolve the temperature gradient in the thermal boundary layer and hence obtain accurate heating rates[28]. These small elements led to very small time steps to meet the stability requirements of the explicit algorithm[30,36]. Although solutions could be obtained, they were impractical and led to the development by Thareja and Morgan [28] of an implicit finite-element cell-centered algorithm and the code LARCNESS, an acronym for Langley Adaptive Remeshing Code and NavEir Stokes Solver. LARCNESS results[28] are in good agreement with the Mach 8 experimental results of Wieting and Holden[34] as shown in Fig. 13. The local pressure (P) and heating rate (Q) distributions, normalized with respect to undisturbed flow stagnation point values, are shown on the right of Fig. 13. The undisturbed (no incident shock) distributions are also shown to emphasize the amplification of the loads. The adaptive unstructured computational mesh shown on the left of Fig. 13 required 8800 nodes, approximately 1/3 the amount required for a stretched but structured mesh[37]. A layer of structured quadrilateral elements, which adapt circumferentially to the otherwise unstructured mesh, are used to capture the boundary layer. The uniformity was required in order to limit eigenvalues required in Roe's averaging technique[28]. Mesh uniformity appears to also be required for current turbulent models, hence turbulence models need to be developed for unstructured meshes as they significantly reduce the computation effort.

Disciplinary Interactions

In all of the examples given, the flow field was coupled to the thermal response of the structure, since the wall temperature affects the amount of energy absorbed from the boundary layer. If the temperature distribution is known a priori then the flow field can be uncoupled from the thermal analysis by specifying the surface temperature distribution. An even stronger coupling occurs when the thermal or mechanical deformations of the structure alter the flow field making an otherwise uniform heating nonuniform or even creating local hot spots.

A metallic thermal protection system (TPS), which consists of 1'x1'x4" tiles mechanically fastened at the corners to a primary structure, glowing from aerodynamic heating (Fig. 14) illustrate this behavior[38]. Prior to aerothermal exposure the TPS is flat. Exposure to the aerodynamic stream causes the tiles to thermally bow into the stream due to the in-depth thermal gradient. Each tile bows approximately spherically creating the quilt like surface shown in Fig. 14. Experimental data[39] and Navier-Stokes analyses[40] showed that the local maximum heating rate(q), equilibrium temperature (T_{eq}), and the total heat flux (Q) were increased above the flat surface value as shown in Fig. 15. The increase was a nonlinear function of the bowed height (h) to boundary layer thickness (δ_{fp}) ratio. In addition, as shown to the left of Fig. 15, the mechanism for the increased heating was a function of the tile alignment (longitudinal and diagonal) and was caused by flow impingement or compression on the protruding tile and vortices generated by the diagonally aligned array. This analysis was performed assuming an isothermal wall and a rigid spherical shape. Although both were reasonable assumptions for the objective of the study, the actual shape and temperature distribution are significantly different as implied by the resulting localized heat flux and temperatures which would alter both the indicated heating rate and the deformations[40].

This type of coupled flow-thermal-structural behavior obviously requires the integrated methodology discussed herein. The current capability in the Langley

Integrated Fluid-Thermal-Structural (LIFTS) analyzer, which uses the Taylor-Galerkin algorithm for all three disciplines, has been demonstrated for the two dimensional equivalent of the bowed TPS array[41]. The actual problem analyzed, shown in Fig. 16, consists of a small panel mounted on a two-dimensional panel holder and exposed to Mach 6.57 flow. The purpose of such a test would be to obtain experimental data for code validation. The panel is simply supported at the lateral edges. This constraint restricts longitudinal thermal growth causing the panel to deflect convexly or concavely, depending on whether the constraint is on the inner or outer surface,respectively. Either deflection alters the aerodynamic flow field causing shock and expansion waves as shown schematically in Fig. 17. The thermal deformations and increased surface temperature both alter the aerodynamic heating distribution as shown in Fig. 18 for the convex panel. The increased wall temperature reduces the heating rate because of the reduced fluid thermal gradient at the wall . However, the heating rate and pressures are increased where the flow is compressed through shock waves (forward part of the panel, See Fig. 17) and decreased where the flow passes through expansion waves (aft part of the panel). The resulting thermal stress distributions are shown in Fig. 19 for the convexly distorted panel.

An experimental heat transfer model representative of a cowl leading edge has also been analyzed[36] with LIFTS. The analysis is for a three inch diameter cylinder immersed in Mach 6.47 flow. The thickness of the cylinder makes the cylinder stiffer than a flight weight leading edge. The flow field analysis[36] is shown in Fig. 20 to compare well with the experimental results of Wieting[33]. The resulting temperature and stress distributions are also given. In this case the thermal deformations are insignificant and do not effect the flow field, which is coupled to the thermal response of the cylinder[36].

The more severe condition of shock-on-lip could not be analyzed with the explicit Taylor-Galerkin algorithm because of the prohibitively small time step[30,36]. The implicit algorithm in LARCNESS is being added to LIFTS as an alternative fluid module to eliminate this shortcoming. The pressure and heating rate distributions based on experimental data[35] were input to LIFTS and an integrated thermal-structural analysis performed on the actively cooled leading edge shown in Fig. 21. Thermal and structural results for shock-on-lip at a simulated Mach 16, 2000 psf dynamic pressure are given in Fig. 22 and 23, respectively. The leading edge is assumed to be made of copper. The copper exhibits thermal super conductivity at cryogenic temperatures[36]. The radial thermal gradients at the impingement point (Fig. 22) of the supersonic jet results in acceptable circumferential stresses as shown in Fig. 23. However, the circumferential thermal gradient (approximately 700 °F) results in axial stresses that exceed the elastic limit of the material. An unexpected benefit of the nonlinear Taylor-Galerkin algorithm developed for the flow analysis is its capability for nonlinear structural analysis[36,41,42]. Temperature dependent stress-strain relations and large deformations are accomodated by updating the finite element matrices during each analysis iteration. A shortcoming of this approach is that rate dependent material effects, which are known to be important at high temperatures, are neglected. Research is currently underway to include such effects using unified viscoplastic theory[43].

Current research is focused on further improvements and evaluation of the various algorithms, turbulence models, chemical equilibrium, adaptive meshing for thermal and structural analysis, hierarchical methods, aposteriori error estimates, and extension to three dimensional for all disciplines.

Concluding Remarks

To meet the analysis requirements for hypersonic vehicles the NASA Langley Research Center is developing the Langley Integrated Fluid-Thermal-Structural (LIFTS) analyzer using finite element techniques. A general automated unstructured gridding is used to discretize the aerodynamic and coolant flow field and the structure for the thermal and structural analyses. Currently a single nonlinear finite element algorithm provides the solution for the environment, loads and response for all three disciplines. The flow field computational domain is adaptively refined based on flow field gradients to minimize grid points and increase accuracy.

The historical development, status, and plans of the integrated fluid-thermal-structural methodology in LIFTS are discussed. The development was initiated in the mid 1970's with the development of a finite element thermal analyzer equivalent to standard finite difference thermal analyzers and interfaced with a structural analyzer. The next step was the development of an integrated thermal-structural analyzer which uses hierarchical elements with nodeless variables. Current research is focused on the development of efficient algorithms and adaptive refinement techniques. The algorithm, developed for the inherently nonlinear fluid equations, has led to unexpected benefits in the solution of nonlinear thermal and structural behavior.

References

[1]Wieting, A. R. and Guy, R. W.: "Thermal-Structural Design of an Airframe-Integrated Hydrogen-Cooled Structures," Journal of Aircraft, Vol. 13, No. 3, pp. 192-197, March, 1976.

[2]Staff of Martin-Marietta Corporation: Martin Interactive Thermal Analyses System, Version 1.0, MDS-SPLPD-71-FD238 (REV3), March, 1972.

[3]Lee, Hwa-Ping and Mason, James B.: Nastran Thermal Analyzer, A General Purpose Finite Element Heat Transfer Computer Program, Nastran User's Experiences, NASA TM X-2637, pp. 443-454.

[4]Wieting, Allan R. and Thornton, Earl A.: "Thermostructural Analysis of a Scramjet Fuel-Injection Strut," Presented at NASA Symposium Advances in Structures for Hypersonic Flight, September 6-8, 1978,

Langley Research Center, Hampton, VA, NASA CP-2065, pp. 851-896, 1978.

[5]Adelman, Howard M. and Robinson, James C.: "Recent Advances in Thermal-Structural Analysis and Design," Presented at NASA Symposium on Recent Advances in Structures and Hypersonic Flight, September 6-8, 1978, NASA Langley Research Center, Hampton, VA, NASA CP-2065, pp. 897-941, 1978.

[6]Thornton, E. A. and Wieting, A. R.: "Comparison of NASTRAN and MITAS Nonlinear Thermal Analyses of a Convectively Cooled Structure," Presented at Fourth NASTRAN User's Colloquium, NASA TM X-3278, NASTRAN User's Experiences, September, 1975.

[7]Thornton, Earl A. and Wieting, Allan R.: "Recent Advances in Thermo-Structural Finite Element Analysis," Presented at NASA Symposium on Recent Advances in Structures and Hypersonic Flight, September 6-8, 1978, NASA Langley Research Center, Hampton, VA, NASA CP-2065, pp. 851-896, 1978.

[8]Thornton, Earl A. and Wieting, Allan R.: "Finite Element Methodology for Transient Conduction/Forced-Convection Thermal Analysis," Presented at the AIAA 14th Thermophysics Conference, Orlando, Florida, June 4-6, 1979, AIAA Paper No. 79-1100.

[9]Thornton, Earl A. and Wieting, Allan R.: "Finite-Element Methodology for Thermal Analysis of Convectively Cooled Structures," Progress in Astronautics and Aeronautics, Vol. 60, Heat Transfer and Thermal Control Systems, Edited by Leroy S. Fletcher, pp. 171-189.

[10]Wieting, Allan R. and Thornton, Earl A.: "Finite Element Thermal Analysis of Convectively-Cooled Aircraft Structures," Numerical Methods in Thermal Problems, Edited by R. W. Lewis, K. Morgan, O. C. Zienkiewicz, John Wiley & Sons Limited, 1980.

[11]Thornton, Earl A. and Wieting, Allan R.: "Finite-Element Methodology for Transient Conduction/Forced-Convection Thermal Analysis," Progress in Astronautics and Aeronautics, Vol. 60, Heat Transfer, Thermal Control, and Heat Pipes, Edited by Walter B. Olstad, pp. 77-103, 1980.

[12]Thornton, E. A. and Wieting, Allan R.: "Evaluation of Finite Element Formulations for Transient Conduction Forced-Convection Analysis," Numerical Heat Transfer, Vol. 3, pp. 281-295, 1980.

[13]Emery, A. F.; Kippenhan, C. J.; Mortazavi, H. and Wieting, A. R.: "Computation of Radiation View Factors for Surfaces with Obstructed View of Each Other," ASME Journal of Heat Transfer, 1981.

[14]Wieting, Allan R. and Thornton, Earl A.: "Finite Element Thermal Analysis of Convectively-Cooled Aircraft Structures," Recent Numerical Advances in Thermal Problems, Chapter 20, pp. 431-443, John Wiley and Sons, Inc., 1981.

[15]Thornton, Earl A. and Wieting, Allan R.: "A Finite-Element Thermal Analysis Procedure for Several Temperature-Dependent Parameters," Transactions of the ASME, Journal of Heat Transfer, Vol. 100, pp. 551-553, August, 1978.

[16]Thornton, Earl A.; Dechaumphai, Pramote and Wieting, Allan R.: "Integrated Thermal-Structural Finite Element Analysis," Presented at the AIAA/ASME/ASCE/AHS 21st Structures, Structural Dynamics and Material Conference, Seattle, WA, May 12-14, 1980. AIAA Paper No. 80-0717-CP.

[17]Thornton, E. A.; Dechaumphai, P. and Wieting, A. R.: "Recent Advances in Finite Element Modeling for Thermal-Structural Analyses," Presented at Symposium on Mathematical Modeling in Structural Engineering, Hampton, VA, October 24-26, 1979.

[18]Thornton, Earl A.; Dechaumphai, Pramote.; Wieting, Allan R. and Tamma, Kumar K.: "Integrated Transient Thermal-Structural Finite Element Analysis," Presented at the AIAA/ASME/ASCE/AHS 22nd Structures, Structural Dynamics and Materials Conference, April 6-8, 1981. AIAA Paper No. 81-0481-CP.

[19]Thornton, Earl A.; Dechaumphai, Pramote and Wieting, Allan R.: "Integrated Finite Element Thermal-Structural Analysis with Radiation Heat Transfer," Presented at the AIAA/ASME/ASCE/AHS 23rd Structures, Structural Dynamics and Materials Conference, New Orleans, Louisiana, May 10-12, 1982, AIAA Paper No. 82-0703-CP.

[20]Thornton, Earl A. and Dechaumphai, Pramote: "A Hierarchical Finite Element Approach for Integrated Thermal Structural Analysis," Presented at the 25th Structures, Structural Dynamics and Materials Conference, May 14-16, 1984, Palm Springs, California, AIAA Paper No. 84-0939-CP.

[21]Ko, W. L., Quinn, R. D., Gong, L., Schuster, L., and Gonzales, D.: "Reentry Heat Transfer Analysis of the Space Shuttle Orbiter," Computational Aspects of Heat Transfer in Structures, pp. 295-325, NASA CP 2216, November 1981 .

[22]Cooke, C. H.: "A Numerical Investigation of the Finite Element Method in Compressible Primitive Variable Navier-Stokes Flow," Old Dominion University Research Foundation, NASA Grant NSG-1098, May, 1977.

[23]Peraire, J.; Morgan, K.; Peiro, J. and Zienkiewicz, O. C.: "An Adaptive Finite Element Method for High Speed Flows," Presented at the AIAA 25th Aerospace Sciences Meeting, Reno, Nevada, January 12-15, 1987, AIAA Paper No. 87-0558.

[24]Thornton, E. A.; Ramakrishnan, R. and Dechaumphai, P.: "A Finite Element Approach for Solutions of the 3D Euler Equations," Presented at the

AIAA 24th Aerospace Sciences Meetings, Reno, Nevada, January 6-8, 1986, AIAA Paper No. 86-0106.

[25]Morgan, K.; Peraire J.; Thareja, R. R. and Stewart, J. R.: "An Adaptive Finite Element Scheme for the Euler and Navier-Stokes Equations," Presented at the AIAA 8th Computational Fluid Dynamics Conference, Honolulu, Hawaii, June 8-10, 1987, AIAA Paper 87-1172.

[26]Thornton, E. A. and Dechaumphai, P.: "Finite Element Prediction of Aerothermal-Structural Interaction of Aerodynamically Heated Panels," Presented at the AIAA 22nd Thermophysics Conference, Honolulu, Hawaii, June 8-10, 1987, AIAA Paper No. 87-1610.

[27]Stewart, J. R.; Thareja, R. R.; Wieting, A. R. and Morgan, K.: "Application of Finite Element and Remeshing Technique to Shock Interference on a Cylindrical Leading Edge," Presented at the AIAA 26th Aerospace Sciences Meeting, Reno, Nevada, January 11-14, 1988, AIAA Paper No. 88-0368.

[28]Thareja, R. R.; Stewart, J. R.; Hassan, O.; Morgan, K. and Peraire, J.: "A Point Implicit Unstructured Grid Solver for the Euler and Navier-Stokes Equations," Presented at the AIAA 26th Aerospace Sciences Meeting, Reno, Nevada, January 11-14, 1988, AIAA Paper No. 88-0036.

[29]Peraire, J.; Peiro, J.; Formaggia, L; Morgan, K. and Zienkiewicz, O. C.: "Finite Element Euler Computations in Three Dimensions," Presented at the AIAA 26th Aerospace Sciences Meeting, Reno, Nevada, January 11-14, 1988, AIAA Paper No. 88-0032.

[30]Ramakrishnan, R.; Bey, K. S. and Thornton, E. A.: "An Adaptive Quadrilateral and Triangular Finite Element Scheme for Compressible Flows," Presented at the AIAA 26th Aerospace Sciences Meeting, Reno, Nevada, January 11-14, 1988, AIAA Paper No. 88-0033.

[31]Hughes, T. R. J.; Franca, L. P.; Harari, I.; Mallet, M.; Shakib, F. and Spelce, T. E.: "Finite Element Method for High speed Flows: Consistent Calculation of Boundary Flux," AIAA 25th Aerospace Sciences Conference, Reno, Nevada, AIAA Paper No. 87-0556, January, 1987.

[32]Edney, B.:"Anomalous Heat Transfer and Pressure Distribution on Blunt bodies at Hypersonic Speeds in the Presence of an Impinging Shock," FFA Rep. 115, Aeronaut. Res. Inst. of Sweden, 1968.

[33]Wieting, A. R.: "Experimental Study of Shock Wave Interference Heating on a Cylindrical Leading Edge," Ph.D. Dissertation, Old Dominion University, Norfolk, Virginia, 1987, also NASA TM-100484, 1987.

[34]Wieting, A. R. and Holden, M. S.: "Experimental Study of Shock Wave Interference Heating on a Cylindrical Leading Edge," Presented at the AIAA 22nd Thermophysics Conference, Honolulu, Hawaii, June 8-10, 1987, AIAA Paper 87-1511.

[35]Holden, M. S., and Wieting, A. R., Moselle, J. R., and Glass, C.: "Studies of Aerothermal Loads Generated in Regions of Shock/Shock Interaction in Hypersonic Flow," Presented at the AIAA 26th Aerospace Sciences Meeting, Reno, Nevada, January 11-14, 1988, AIAA Paper No. 88-0477.

[36]Dechaumphai, P., Thornton, E.A., Wieting, A.R.: "Flow-Thermal-Structural Study of Aerodynamically Heated Leading Edges," Presented at the AIAA/ASME/ASCE/AHS 29th Structures, Structural Dynamics and Materials Conference, Williamsburg, VA., April 18-20, 1988, AIAA Paper No. 88-2245-CP.

[37]G. H. Klopfer and H. C. Yee: "Viscous Hypersonic Shock on Shock Interaction on Blunt Cowl Lips," Presented at the AIAA 26th Aerospace Sciences Meeting, Reno, Nevada, January 11-14, 1988, AIAA Paper 88-0233.

[38]Shideler, J. L., Webb, G. L. and Pittman, C. M.: "Verification Tests of Durable Thermal Protection System Concepts," Journal of Spacecraft and Rockets, Vol. 22, No. 6, November 1985, pp. 598-604.

[39]Glass, C. E. and Hunt, L. R.: "Aerothermal Tests of Quilted Dome Models on a Flat Plate at a Mach Number of 6.5," May, 1988, NASA Technical Paper 2804.

[40]Olsen, G. C., and Smith, R. E.: "Analysis of Aerothermal Loads on Spherical Dome Protuberances," AIAA Journal, Vol. 23, No. 5, May 1985, pp. 650-656.

[41]Thornton, E. A. and Dechaumphai, P.: "Coupled Flow, Thermal and Structural Analysis of Aerodynamically Heated Panels," Presented at the AIAA/ASME/AHS 28th Structures, Structural Dynamics and Materials Conference, Monterey, California, April 6-8, 1987, AIAA Paper No. 87-0701-CP.

[42]Thornton, E. A. and Dechaumphai, P.: "A Taylor-Galerkin Finite Element Algorithm for Transient Nonlinear Thermal-Structural Analysis," Presented at the AIAA/ASME/AHS 27th Structures, Structural Dynamics and Materials Conference, San Antonio, Texas, May 19-21, 1986, AIAA Paper No. 86-0911-CP.

[43]Bodner, S. R.: "Review of a Unified Elastic-Viscoplastic Theory," Unified Constitutive Equations for Creep and Plasticiy, edited by Miller, A. K., Elsvier Applied Science Pub., England, 1987.

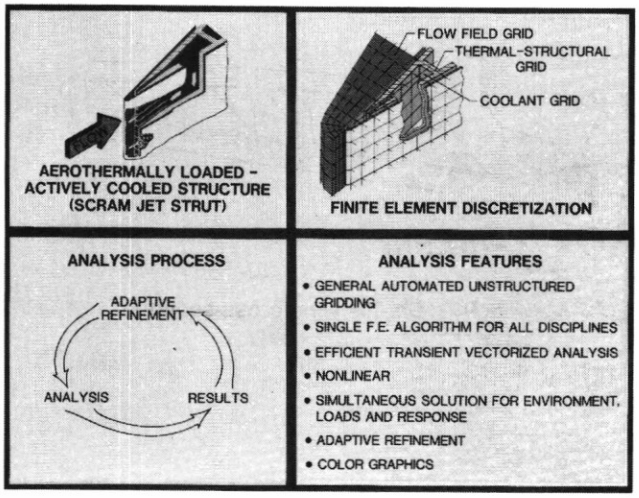

Fig. 1 Illustration of Langley Integrated Fluid-Thermal-Structural Finite Element Analysis Procedure.

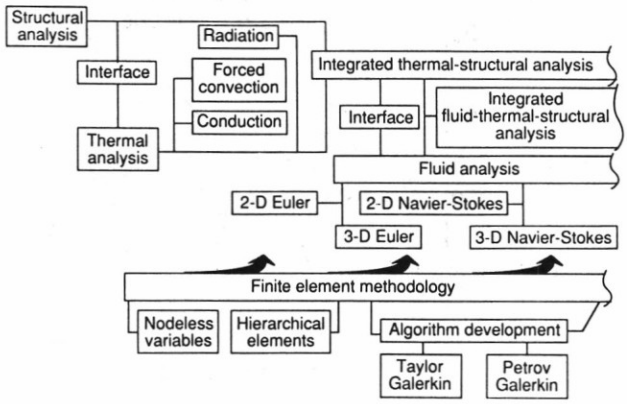

(a) Past and Present

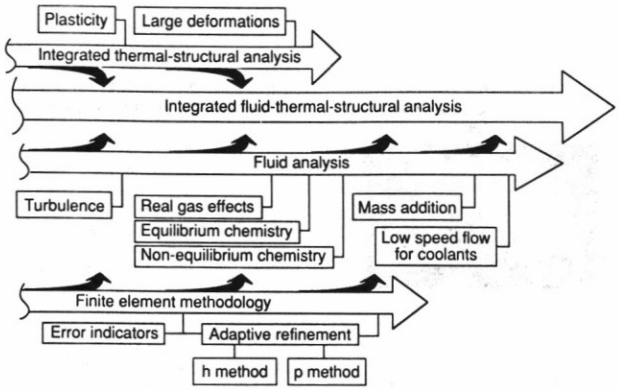

(b) Future

Fig. 2 Past, Present, and Future development of integrated finite element methods in LIFTS.

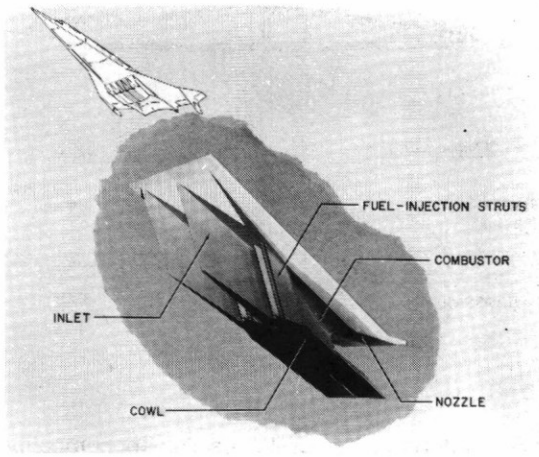

Fig. 3 Airframe-integrated supersonic combustion ramjet.

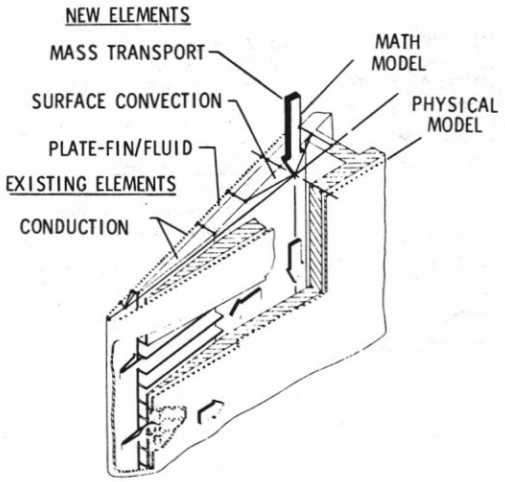

Fig. 4 Thermal element development for actively cooled structure.

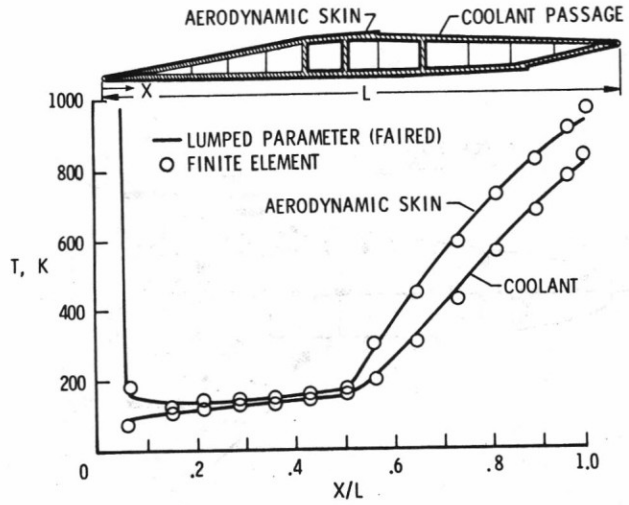

Fig. 5 Comparison of finite element and finite difference techniques in predicting thermal response of an actively cooled strut.

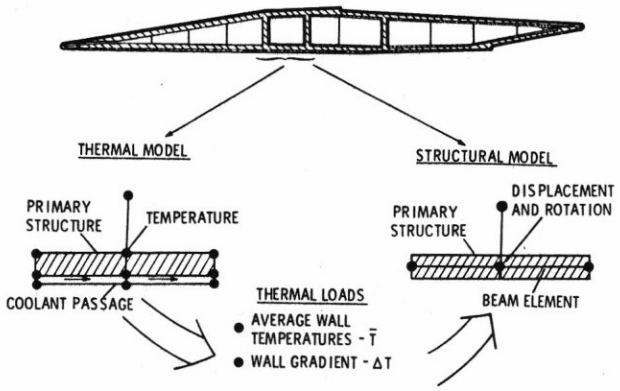

Fig. 6 Thermal-structural finite element compatibility.

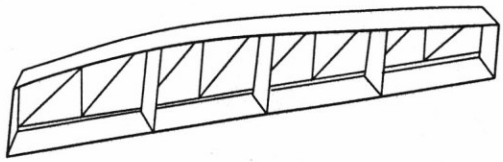

Fig. 9 Shuttle wing cross-section.

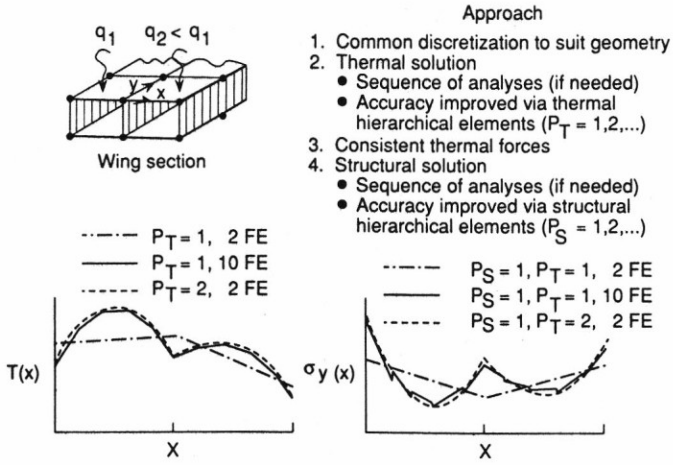

Fig. 7 Integrated thermal structural analysis with hierarchical thermal elements with nodeless variables.

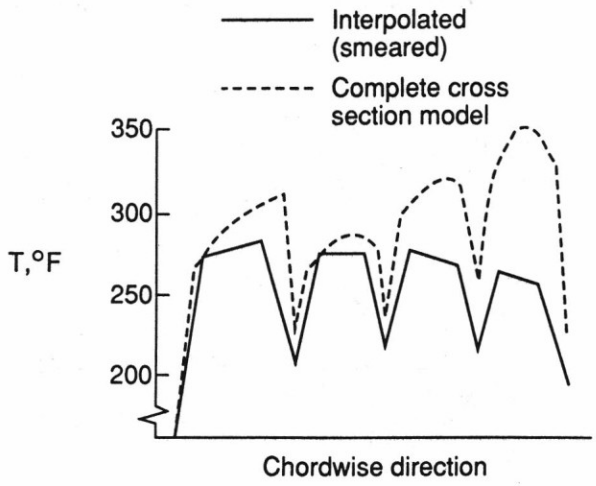

Fig. 10 Comparison of interpolated temperatures with detailed cross section temperatures.

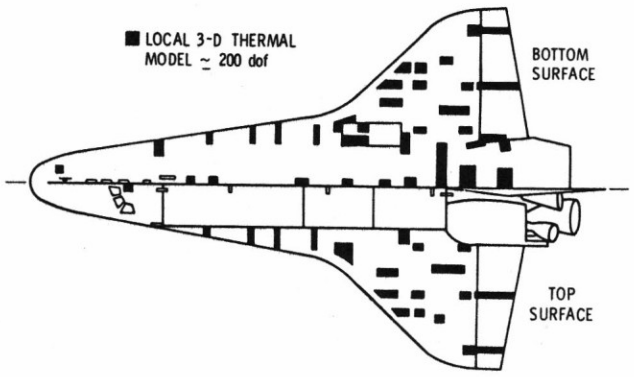

Fig. 8 Three dimensional plug model location for shuttle thermal analysis.

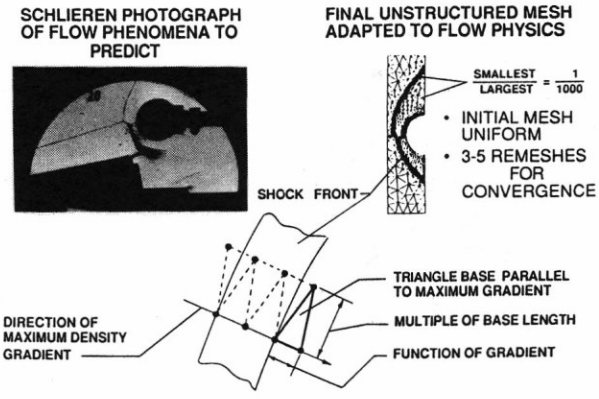

Fig. 11 Adaptive unstructured remeshing scheme.

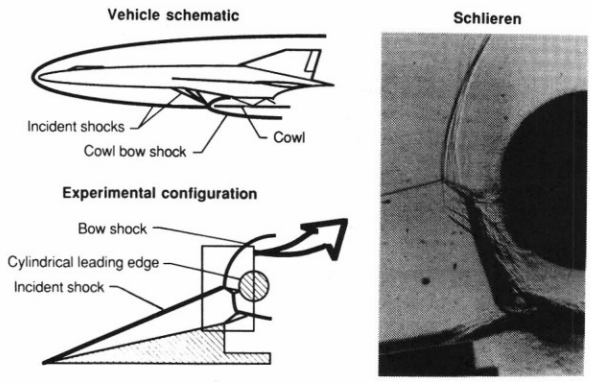

Fig. 12 Shock-on-lip interference phenomena.

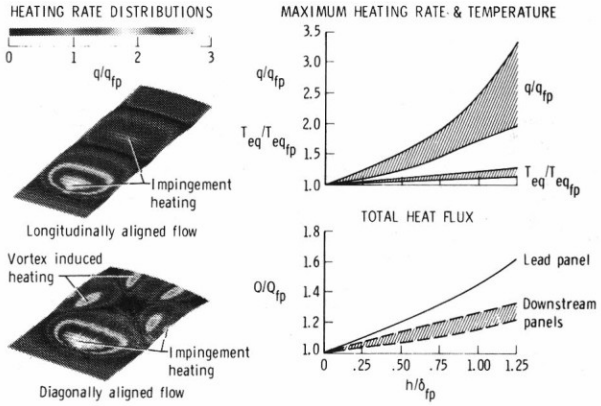

Fig. 15 Navier-Stokes analysis of thermally bowed TPS showing augmented thermal loads.

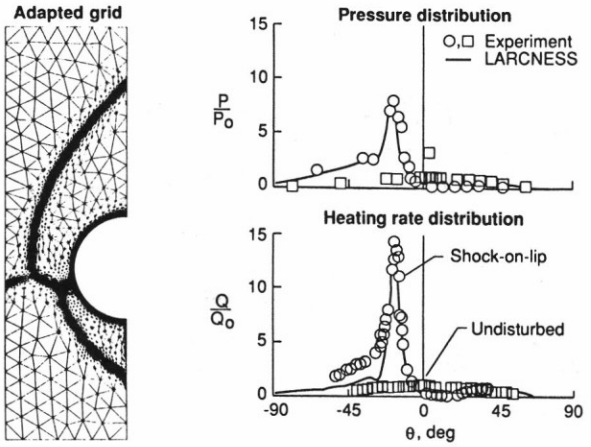

Fig. 13 LARCNESS adapted grid and comparison with experiment.

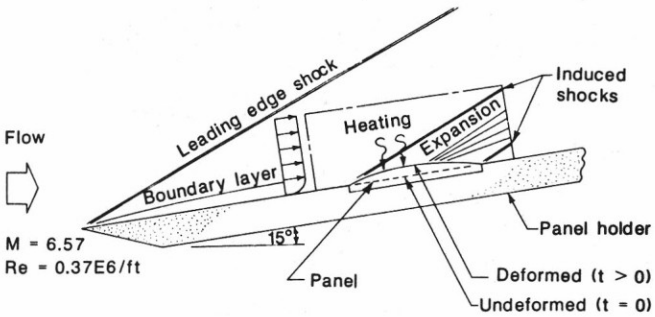

Fig. 16 Schematic of aerodynamically heated panel thermally bowing into flow field.

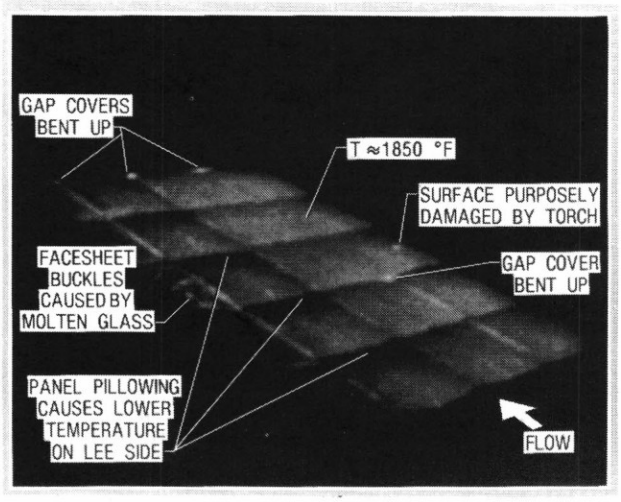

Fig. 14 Metallic TPS deformed during aerothermal exposure at Mach 7.

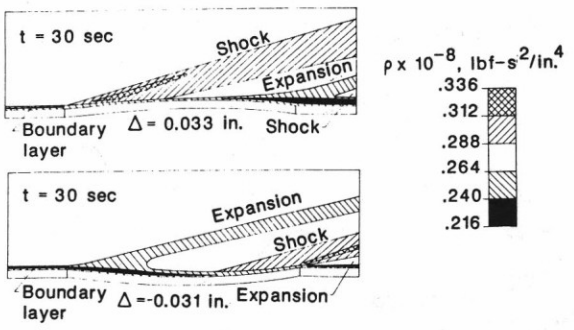

Fig. 17 Schematic showing interaction of convex and concave panel deflections on aerodynamic flow.

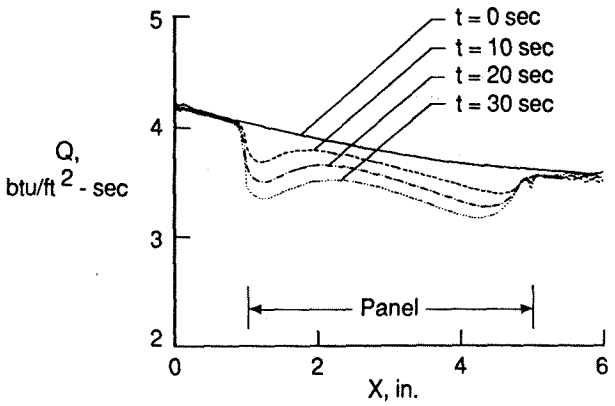

Fig. 18 Effect of surface temperature distribution and deformations on the panel heating rate distribution.

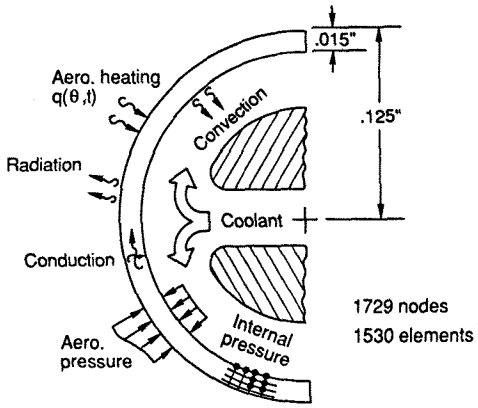

Fig. 21 Schematic of actively cooled cylindrical leading edge.

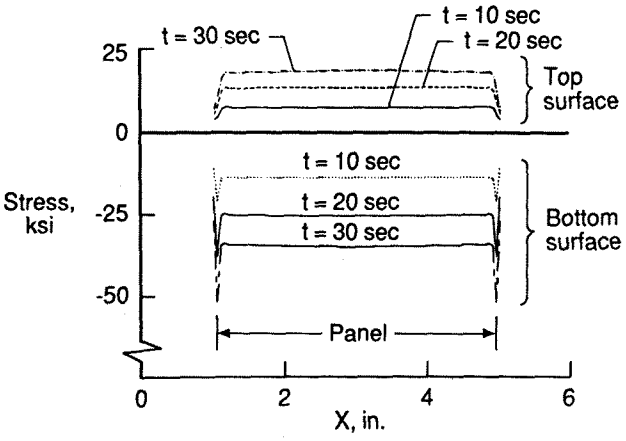

Fig. 19 Panel thermal stress distributions corresponding to heating rates at different times.

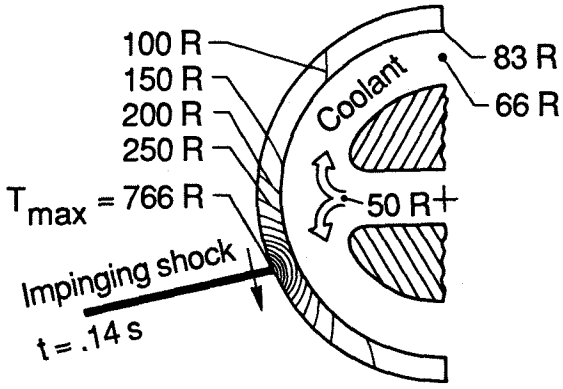

Fig. 22 Thermal response of leading edge with shock-on-lip.

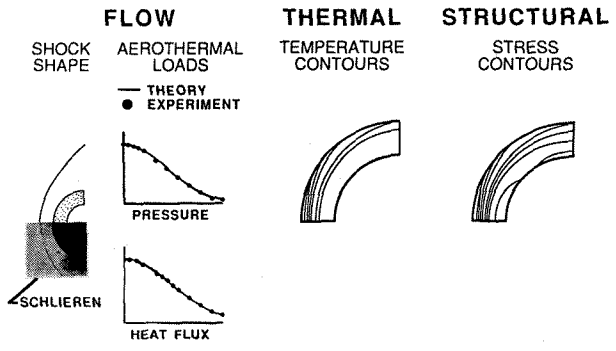

Fig. 20 Flow-thermal-structural behavior of a cylindrical leading edge as predicted by LIFTS.

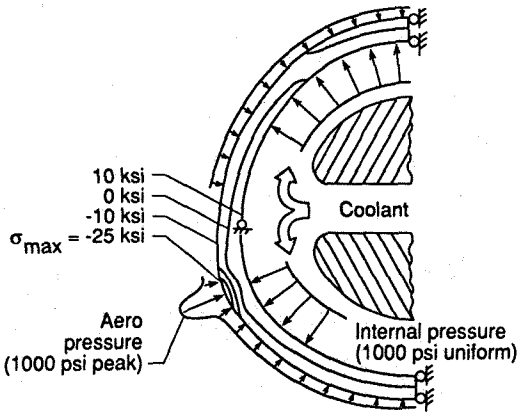

Fig. 23 Circumferential thermal and mechanical stress distribution in leading edge.